



ACADÉMIE
DES SCIENCES
INSTITUT DE FRANCE

Comptes Rendus

Chimie

Noureddine EL Hasbaoui, Abdelouahab EL Hadrami and Rachid Brahmi

Accelerated deactivation of industrial SO₂ oxidation catalysts in sulfuric acid production

Volume 29 (2026), p. 99-105

Online since: 25 February 2026

<https://doi.org/10.5802/crchim.432>

 This article is licensed under the
CREATIVE COMMONS ATTRIBUTION 4.0 INTERNATIONAL LICENSE.
<http://creativecommons.org/licenses/by/4.0/>



*The Comptes Rendus. Chimie are a member of the
Mersenne Center for open scientific publishing*
www.centre-mersenne.org — e-ISSN : 1878-1543



Research article

Accelerated deactivation of industrial SO₂ oxidation catalysts in sulfuric acid production

Noureddine EL Hasbaoui^{✉,*}, Abdelouahab EL Hadrami^{✉,a} and Rachid Brahmi^{✉,a}

^a Coordination and Analytical Chemistry Laboratory (LCCA), Department of Chemistry, Faculty of Sciences, Chouaïb Doukkali University, El Jadida, Morocco
E-mail: elhasbaoui.n@ucd.ac.ma (N. EL Hasbaoui)

Abstract. This study investigates the forced deactivation of fresh catalyst used in sulfuric acid production through exposure to water vapor with the objective of gaining deeper insight into the mechanisms of catalytic deactivation for a short duration (up to 4 h). An experimental procedure was developed to reproduce deactivation phenomena under controlled conditions, considering key parameters such as temperature, SO₂/N₂ ratio, and steam presence, to assess their effects on catalyst structure and catalytic performance. The commercial V₂O₅-M₂SO₄/SiO₂ catalyst widely employed in H₂SO₄ production is known to progressively lose efficiency over time, with complete inactivation occurring after approximately 10 years of service, depending on the catalytic mass. Catalyst deactivation is typically linked to chemical, mechanical, and thermal factors. In this work, steam-induced deactivation was simulated using a dedicated test bench, with precise control of SO₂ and N₂ flow rates via needle control valves to achieve SO₂/N₂ ratios of 0.84 and 1.65. The water bath temperature was maintained at 80 °C while the reaction temperature was controlled at 350 °C. The reaction time was also investigated as a critical factor influencing deactivation. Catalysts subjected to these conditions were analyzed using XRF, XRD, and FTIR techniques. Their performance was further validated by catalytic testing of SO₂ oxidation to SO₃, with iodometric titration used to quantify reactivity. The results revealed significant structural modifications accompanied by a marked decrease in catalytic activity to approximately 36% from an initial conversion rate of about 63%.

Keywords. Sulfuric acid, Oxidation of SO₂, Industrial vanadium-based catalyst, Catalyst deactivation.

Funding. OCP Foundation (APPHOS project).

Note. Submitted by invitation as part of the 13th edition of the Moroccan Meetings on Solid State Chemistry (REMCES-13).

Manuscript received 22 June 2025, revised 9 October 2025, accepted 19 November 2025, online since 25 February 2026.

1. Introduction

Sulfuric acid is, thus far, one of the most widely used mineral products across various fields, particularly in the chemical industry for the production of phosphoric acid and fertilizers. The manufacturing process of sulfuric acid relies on three main steps: (1) the combustion of liquid sulfur, (2) the oxidation of sulfur dioxide to sulfur trioxide, and (3) the absorption

of SO₃ with water to form H₂SO₄. The conversion reaction from SO₂ to SO₃, also known as the contact process [1,2], is a crucial step in sulfuric acid production. Its very high activation energy leads to a slow reaction rate and low conversion efficiency; therefore, catalysts are required to lower the energy barrier. The vanadium-based catalyst used is deposited on a silica or alumina support to increase the contact effect with the substrate, and it is mixed with alkaline promoters typically potassium, sodium, and/or cesium [3]. During the oxidation of SO₂ to SO₃, the vanadium-based catalyst becomes active at around 420 °C [4] and

*Corresponding author

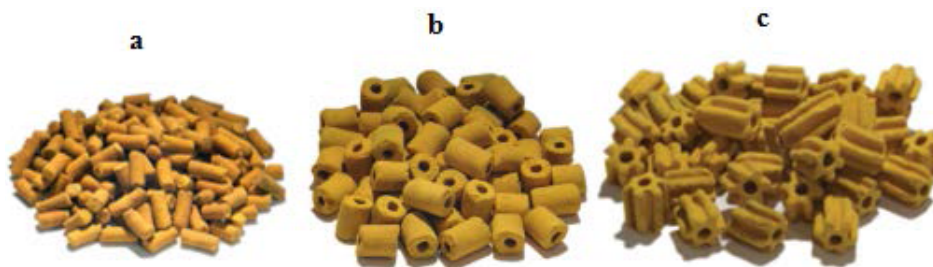
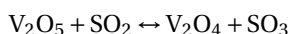


Figure 1. Differently shaped catalysts proposed by MECS (USA): (a) extruded, (b) rings, and (c) stars.

operates according to a redox cycle mechanism [2,5] as illustrated by the following equation:



The primary issues with the catalyst during multiple cycles of SO_2 to SO_3 oxidation eventually lead to a decrease in its activity, indicating deactivation and/or aging of the catalyst. In addition, there is a gradual increase in pressure due to high operating temperatures and the dust carried by the gases as well as surface poisoning and pore blockage. To restore the catalyst's activity, regeneration processes can be applied; however, in some cases, the catalyst must be replaced with a new one. Deactivated catalysts are classified as hazardous waste [6].

Several studies have investigated the thermal deactivation of vanadium-based catalysts used in the SO_2 oxidation reaction [7–10]. Lapina et al. [7] studied the influence of reagents on SO_2 conversion and reported that the deactivation is partly attributed to structural changes in both the support and the active phase, leading to the formation of new non-active phases, particularly vanadyl sulfates.

Akola et al. [11] investigated catalyst deactivation caused by fine particle formation, which occurs more rapidly with decreasing vanadium content in the catalyst accompanied by structural changes and the formation of sulfated compounds. Grobela and Grzesiak [12] reported additional noteworthy findings, explaining that the presence of iron oxide in the active phase of the catalyst promotes the oxidation of SO_2 to SO_3 at temperatures above 600°C , whereas iron sulfate contributes to catalytic deactivation and may even lead to an increase in temperature.

The aim of this study is to investigate the accelerated deactivation of industrial catalysts by water vapor in the shortest possible time in order to

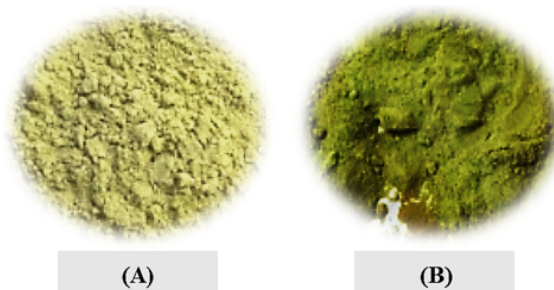


Figure 2. (A) Fresh catalyst and (B) deactivated catalyst.

gain a deeper understanding of the mechanism. The deactivated catalysts were characterized using various techniques such as X-ray fluorescence (XRF), X-ray diffraction (XRD), and Fourier transform infrared (FTIR) spectroscopy. Their catalytic performance was subsequently evaluated through catalytic testing to assess the effect of water vapor on activity.

2. Materials and methods

2.1. Materials

The study was carried out using commercial vanadium-based catalysts supplied by MECS (USA). These catalysts are manufactured in different geometric shapes, the most common being extrudates, rings, and stars (Figure 1) [13]. Figure 2 illustrates the physical appearance of fresh and deactivated catalysts: the fresh catalyst exhibits a yellow color, whereas the deactivated catalyst appears green. This color change is attributed to structural modifications induced during the accelerated deactivation treatment.

2.2. Leaching process

The fresh catalyst was ground in a porcelain mortar, and 300 mg of the resulting powder was weighed

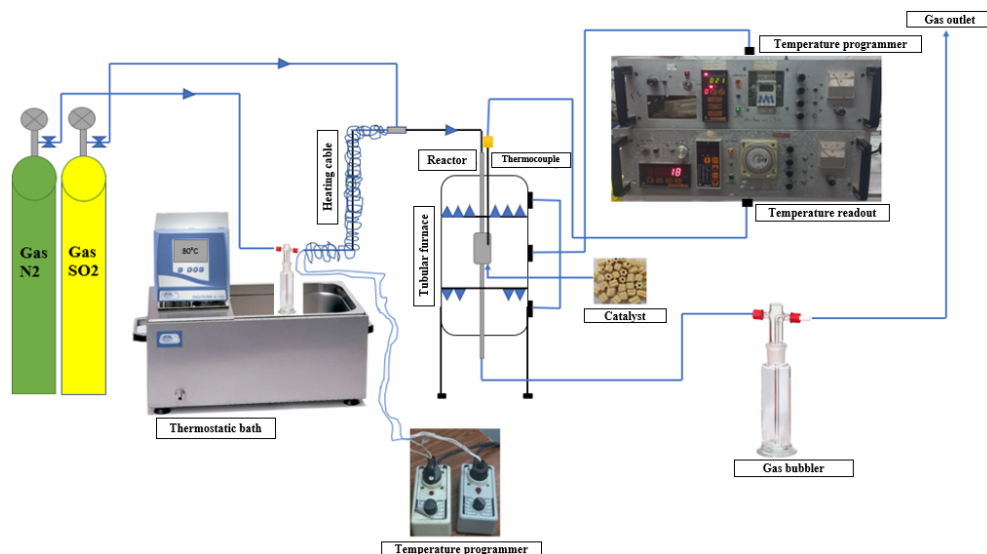


Figure 3. Accelerated deactivation in a steam and SO₂ deactivation setup.

Table 1. The operating conditions for catalyst deactivation

Designation	Reaction temperature (°C)	N ₂ flow rate (mL/min)	SO ₂ flow rate (mL/min)	SO ₂ /N ₂ ratio	Reaction time (h)
Deactivated catalyst	350	71	60	0.85	2
Deactivated catalyst	350	26	43	1.65	4

and introduced into a tubular glass reactor equipped with two inlets (Inlet 1: SO₂; Inlet 2: steam + N₂) and a glass frit to support the catalyst. The reactor fitted with a thermowell containing a thermocouple was placed as close as possible to the catalyst for precise temperature monitoring. The tubular furnace was connected to a temperature controller to regulate the reaction temperature. At the furnace inlet, steam was generated using a bubbler filled with water maintained at 80 °C in a thermostatic bath. This steam was carried by nitrogen, with the steam circuit being surrounded by a heating cord to prevent condensation. The resulting steam, mixed with SO₂, passed through the catalyst bed at 350 °C for varying time periods. The outlet gases were directed through a bubbler before being released (Figure 3).

2.3. Characterization techniques

The chemical composition of fresh, spent, and deactivated industrial catalyst was determined by XRF analysis using a Bruker AXS S2 Puma EDXRF

spectrometer equipped with a silver anticathode. The crystalline phases were then identified by XRD, using a Bruker Advance diffractometer with a Cu-K α radiation source ($\lambda = 1.5418 \text{ \AA}$). Finally, FTIR spectroscopy was employed to investigate the surface chemistry of the catalysts and to confirm the phases identified by XRD. Infrared transmission spectra were recorded on a Nicolet Impact 400D spectrometer in the range of 500 to 4000 cm⁻¹.

2.4. Experimental conditions

The forced deactivation of the catalysts was carried out by exposing them to a mixture of SO₂ and H₂O vapors at different ratios to simulate the conditions under which catalysts are exposed to sulfur compounds and to better understand the deactivation process. The poisoning treatments consisted of exposing the fresh catalyst to a reaction mixture of SO₂ and steam at a temperature below that of the SO₂ to SO₃ oxidation reaction (approximately 350 °C). The operating conditions applied for the deactivation experiments are summarized in Table 1.

Table 2. Chemical composition of fresh, spent, and deactivated catalysts, at different ratios, analyzed by XRF

Item description	Fe ₂ O ₃	CaO	K ₂ O	SO ₃	SiO ₂	V ₂ O ₅
Fresh catalyst (%)	1.8	0.50	13.78	21.11	52.32	8.48
Spent catalyst (%)	1.18	0.13	8.76	19.40	65.23	4.40
Deactivated catalyst (SO ₂ /N ₂) = 1.66	1.94	0.49	16.02	28.32	43.60	9.64
Deactivated catalyst (SO ₂ /N ₂) = 0.85	2.12	0.68	17.12	27.07	42.62	10.38

2.5. Iodometric determination

The catalytic performance of both fresh and deactivated catalysts was evaluated under simulated industrial conditions, reproducing those of the sulfuric acid production units at Jorf Lasfar. The evaluation was based on an iodometric back-titration method, which enables the quantification of unconverted SO₂ and thus the determination of the catalytic conversion rate. In this approach, the outlet gas stream was passed through a 0.1 mol·L⁻¹ iodine solution, where SO₂ reacts with iodine to form sulfate ions (SO₂ + I₂ + 2H₂O → SO₄²⁻ + 4H⁺ + 2I⁻) [14]. The residual iodine was subsequently titrated with a standardized 0.1 mol·L⁻¹ sodium thiosulfate solution according to the following half-equations: I₂ (aq) + 2e⁻ → 2I⁻ (aq) and 2S₂O₃²⁻ (aq) → S₄O₆²⁻ (aq) + 2e⁻, which combine to give the overall reaction I₂ (aq) + 2S₂O₃²⁻ (aq) → S₄O₆²⁻ (aq) + 2I⁻ (aq). Based on these stoichiometric relations, the amount of unconverted SO₂ was calculated using the expression $n(\text{SO}_2)_{\text{unreacted}} = n(\text{I}_2)_{\text{initial}} - n(\text{I}_2)_{\text{titrated}}$. The catalytic tests were performed using 300 mg of catalyst at a reaction temperature of 450 °C, with both iodine and sodium thiosulfate solutions standardized at 0.1 mol·L⁻¹.

3. Results and discussion

3.1. Characterization of fresh, spent, and deactivated catalysts

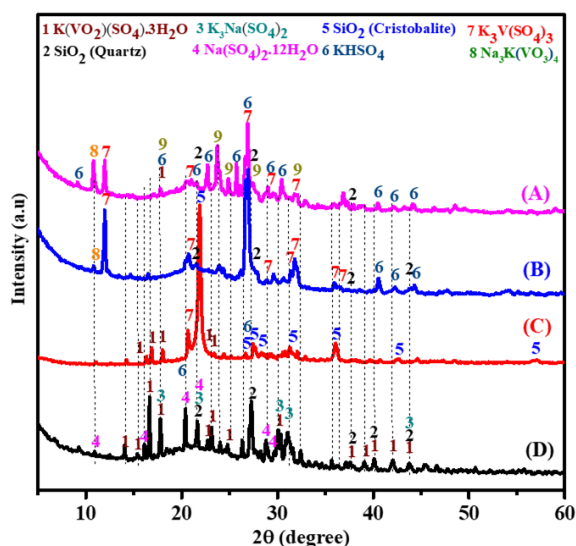
The XRF analysis provided insights into the evolution of the chemical composition of the catalysts after forced deactivation. The results (Table 2) revealed an average increase of 24% in the concentrations of iron (Fe), calcium (Ca), potassium (K), sulfur (S), and vanadium (V) in the active phases. This indicates a change in the percentage composition of the catalyst after deactivation, mainly due to the increase

in sulfur (S) content among these elements in the catalyst residues following deactivation. In contrast, the concentration of these elements increased in the active catalyst residues after deactivation. The silicon (Si) content decreased by 18%, indicating possible degradation or loss of this component during the deactivation process (Table 2). The deactivated catalysts exhibit a high content of potassium, sodium, and sulfur, which react with vanadium to form compounds such as K₃V(SO₄)₃ and Na₃K(VO₃)₄. This involves the reduction of V⁵⁺ present in the fresh catalyst phase K(VO₂)(SO₄)·3H₂O [15] to V³⁺. Silica is also identified in the deactivated catalyst, as evidenced by the XRD patterns showing characteristic peaks (index no. 2), although a large portion remains in the amorphous phase (Figure 4). At temperatures between 205 °C and 370 °C, SO₃ vapors react with water vapors to form H₂SO₄ aerosols. These aerosols can condense or deposit on the catalyst surface, initiating reactions that alter both the phases and the physicochemical properties of the catalyst [16]. Such modifications are primarily responsible for catalyst deactivation [11]. Furthermore, it was observed that when the SO₂/N₂ ratio decreases relative to the catalytic activity, the presence of additional water molecules promotes catalyst degradation, leading to the formation of inactive species such as V³⁺.

The FTIR spectroscopy was employed to analyze the catalyst samples, providing detailed information on the chemical bonds and molecular vibrations present (Figure 5). As shown in Table 3, the planar rotations of V–O–V bonds observed at 550 and 670 cm⁻¹ are characteristic of vanadium-containing compounds [17–19], reflecting specific interactions between vanadium and oxygen atoms within the crystal lattice. The band around 798 cm⁻¹ corresponds to asymmetric V–O–V stretching vibrations [11]. A band near 874 cm⁻¹, also attributed to V–O–V vibrations [20], together with the band at

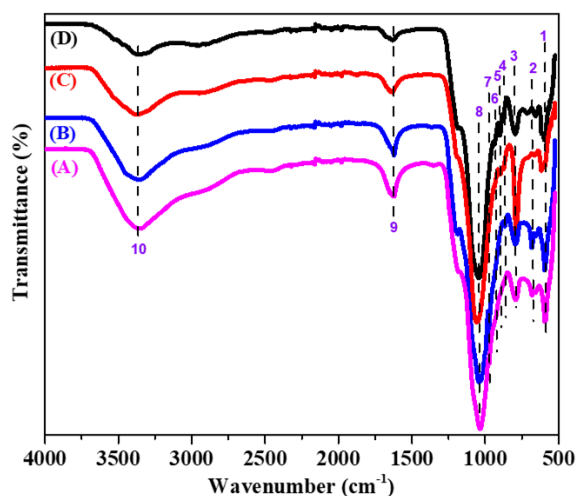
Table 3. FTIR bands characteristic of the different catalyst bands

N ^o .	Position (cm ⁻¹)	Type of chemical bond
1–2	550 and 670	Planar rotation of V–O–V bonds
3	797	Symmetric vibration of Si–O–Si
4	874	Vibration of the V–O–V link
5	900	V–O–S link vibration
6	933	Si–O–V bonding vibration
7	975	V=O vibration of polymerized vanadate species
8	1060	Asymmetric elongation vibration of the Si–O–Si band
9	1643	Bond elongation vibration (H–O–H)
10	3380	Vibration of the (O–H) bond

**Figure 4.** X-ray diffraction patterns of the fresh catalyst (D), the spent catalyst (C), and deactivated catalyst obtained in SO₂/N₂ ratios of 0.85 (B) and 1.66 (A).

900 cm⁻¹, assigned to V–O–S vibrations, confirms the presence of vanadium–oxygen complexes. The band observed at 933 cm⁻¹ indicates Si–O–V interactions [21] while the band at 975 cm⁻¹, assigned to V=O stretching of polymerized vanadate species [22], suggests polymerization of vanadate compounds within the catalyst.

In addition, a broad band at around 1060 cm⁻¹, corresponding to asymmetric Si–O–Si stretching vibrations, indicates the presence of extended siliceous structures [17,23,24]. A band in the 1020–1070 region is associated with sulfate stretching or V–O–SO₄ vi-

**Figure 5.** FTIR spectra of the fresh catalyst (D), the spent catalyst (C), and the deactivated catalyst obtained in SO₂/N₂ ratios of 0.85 (B) and 1.66 (A).

brations [25]. The band at 1643 cm⁻¹ is attributed to the bending vibrations of adsorbed water [26]. Finally, a broad band in the 3720–2600 cm⁻¹ region, assigned to surface hydroxyl groups and coordinated water molecules [26,27], was also observed. These FTIR spectroscopic results are consistent with the phases identified by XRD and confirmed by XRF, providing a comprehensive understanding of the chemical composition and structural features of the catalysts. Such information is crucial for elucidating the mechanisms of catalyst operation and deactivation as well as for guiding regeneration strategies and improving catalytic performance.

Table 4. Measured conversion rates for different catalysts

Designation	Ratio (SO ₂ /N ₂)	Reaction time (h)	Conversion rate
Fresh catalyst			63
Deactivated catalyst	1.65	4	44
Deactivated catalyst	0.85	2	36

3.2. Catalytic test

A catalytic test was carried out on the SO₂ to SO₃ conversion reaction to confirm the results obtained in this study. This test allows the practical efficiency of the catalysts to be evaluated under conditions close to industrial reality. The results (Table 4) show a rapid decrease in the activity of the deactivated catalyst compared to the fresh catalyst, with a SO₂/N₂ ratio of 0.85 after only 2 h of reaction. This loss of performance can be attributed to several factors related to the structural and chemical modifications of the catalyst. Characterization of the deactivated catalyst by FTIR, XRF, and XRD confirmed a reduction in the SiO₂ support and an enrichment in vanadium and sulfur phases, leading to the formation of less active compounds for the SO₂ to SO₃ conversion step. In particular, the appearance of the K₃V(SO₄)₃ and Na₃K(VO₃)₄ phases containing vanadium in the +3 oxidation state, which is less active than the +5 state of the initial vanadium phases, contributes significantly to the decline in catalytic performance, as confirmed by the study reported by Eriksen et al. [8]. The catalytic test results therefore confirm that the structural and chemical modifications occurring during deactivation have a direct impact on catalyst efficiency. Overall, these findings highlight the importance of understanding and controlling deactivation mechanisms in order to improve catalyst durability and performance in industrial applications. The data obtained provide a solid basis for developing regeneration and optimization strategies aimed at extending catalyst lifetime and maintaining high efficiency in sulfuric acid production processes.

4. Conclusion

In this work, forced deactivation was investigated in order to elucidate the main causes of industrial catalyst deactivation during sulfuric acid production over a short timescale. Deactivation by

water vapor was observed when the SO₂/N₂ ratio decreases, leading to visible color change accompanied by structural modification of the catalyst. The XRF analysis revealed an enrichment in active elements and a reduction in the silica support, together with the formation of less active vanadium species in the +3 oxidation state (V³⁺), which are associated with the loss of catalytic activity.

Sulfate accumulation was also evidenced with XRD confirming the development of new sulfate phases. This finding was supported by FTIR analysis, which showed increased sulfate deposition on the deactivated catalyst surface due to adsorption of SO₂ and SO₃ as well as higher water molecule interactions, leading to phase transformations responsible for catalyst deactivation.

Catalytic testing confirmed these structural and chemical changes, showing that activity was reduced by nearly half with the conversion dropping from an initial 63% to 36% after 2 h of operation at 350 °C in the SO₂/N₂ ratio of 0.85.

Acknowledgments

The authors would like to express their sincere gratitude to the OCP Foundation for funding the APPHOS project.

Declaration of interests

The authors do not work for, advise, own shares in, or receive funds from any organization that could benefit from this article, and have declared no affiliations other than their research organizations.

References

- [1] W. G. Davenport and M. J. King, "Chapter 7 - Catalytic oxidation of SO₂ to SO₃", in *Sulfuric Acid Manufacture* (W. G. Davenport and M. J. King, eds.), Elsevier: Oxford, 2006, pp. 71–88.

- [2] J. P. Dunn, H. G. Stenger and I. E. Wachs, "Molecular structure–reactivity relationships for the oxidation of sulfur dioxide over supported metal oxide catalysts", *Catal. Today* **53** (1999), pp. 543–556.
- [3] H. F. Rase, *Handbook of Commercial Catalysts: Heterogeneous Catalysts*, 1st edition, CRC Press: Boca Raton, FL, 2000.
- [4] P. Trambouze and J.-P. Euzen, *Les Réacteurs chimiques; De la conception à la mise en oeuvre*, Ed. Technip: Paris, 2002.
- [5] P. Mars and J. G. H. Maessen, "The mechanism and the kinetics of sulfur dioxide oxidation on catalysts containing vanadium and alkali oxides", *J. Catal.* **10** (1968), pp. 1–12.
- [6] M. Marafi and A. Stanislaus, "Spent catalyst waste management: a review: Part I—Developments in hydroprocessing catalyst waste reduction and use", *Resour. Conserv. Recycl.* **52** (2008), pp. 859–873.
- [7] O. B. Lapina, B. S. Bal'zhinimaev, S. Boghosian, K. M. Eriksen and R. Fehrmann, "Progress on the mechanistic understanding of SO₂ oxidation catalysts", *Catal. Today* **51** (1999), pp. 469–479.
- [8] K. M. Eriksen, D. A. Karydis, S. Boghosian and R. Fehrmann, "Deactivation and compound formation in sulfuric-acid catalysts and model systems", *J. Catal.* **155** (1995), pp. 32–42.
- [9] A. Christodoulakis and S. Boghosian, "Molecular structure of supported molten salt catalysts for SO₂ oxidation", *J. Catal.* **215** (2003), pp. 139–150.
- [10] S. G. Masters, A. Chrissanthopoulos, K. M. Eriksen, S. Boghosian, R. Fehrmann and C. Activity, "Deactivation of SO₂ oxidation catalysts in simulated power plant flue gases", *J. Catal.* **166** (1997), pp. 16–24.
- [11] J. Akola, P. Unnikrishnan, M. B. Joshi, P. K. Chinthala and B. Dhaduk, "Insight studies on the deactivation of sulfuric acid regeneration catalyst", *J. Indian Chem. Soc.* **101** (2024), article no. 101140.
- [12] M. Grobela and P. Grzesiak, "The influence of iron compounds in the sulfuric acid catalyst on the SO₂ oxidation process", *Pol. J. Chem. Technol.* **9** (2007), pp. 2–6.
- [13] D. K. Louie, *Handbook of Sulphuric Acid Manufacturing*, DKL Engineering, Inc: Thornhill, 1961.
- [14] N. Badri, Y. Chhiti, F. Bentiss and M. Bensitel, "Synthesis and characterization of vanadium pentoxide on different metal oxides by the sol–gel process for application in the conversion of the SO₂ to SO₃", *Mor. J. Chem.* **8** (2020), no. 3, pp. 560–572.
- [15] N. El Hasbaoui, A. EL Hadrami, K. Essifi, J. Assaoui and R. Brahmi, "Recycling of spent catalysts used in sulfuric acid production", *Mor. J. Chem.* **13** (2025), pp. 405–423.
- [16] R. J. Jaworowski and S. S. Mack, "Evaluation of methods for measurement of SO₃/H₂SO₄ in Flue Gas", *J. Air. Pollut. Control. Assoc.* **29** (1979), pp. 43–46.
- [17] G. N. Barbosa and H. P. Oliveira, "Synthesis and characterization of V₂O₅–SiO₂ xerogel composites prepared by base catalysed sol–gel method", *J. Non-Cryst. Solids* **352** (2006), pp. 3009–3014.
- [18] V. Iannazzo, G. Neri, S. Galvagno, M. Di Serio, R. Tesser and E. Santacesaria, "Oxidative dehydrogenation of isobutane over V₂O₅-based catalysts prepared by grafting vanadyl alkoxides on TiO₂–SiO₂ supports", *Appl. Catal. A Gen.* **246** (2003), pp. 49–68.
- [19] A. Comite, A. Sorrentino, G. Capannelli, M. Di Serio, R. Tesser and E. Santacesaria, "Oxidative dehydrogenation of propane using V₂O₅/TiO₂/SiO₂ catalysts prepared by grafting titanium and vanadium alkoxides on silica", *J. Mol. Catal. A Chem.* **198** (2003), pp. 151–165.
- [20] L. J. Burcham, G. Deo, X. Gao and I. E. Wachs, "In situ IR, Raman, and UV–Vis DRS spectroscopy of supported vanadium oxide catalysts during methanol oxidation", *Top. Catal.* **11** (2000), pp. 85–100.
- [21] V. Murgia, E. M. F. Torres, J. C. Gottifredi and E. L. Sham, "Sol–gel synthesis of V₂O₅–SiO₂ catalyst in the oxidative dehydrogenation of n-butane", *Appl. Catal. A Gen.* **312** (2006), pp. 134–143.
- [22] M. Ismail, A. Ali and S. Thahab, "Synthesis of vanadium oxide nanoparticles/Psi heterojunction photodetector", *Charact. Appl. Nanomater.* **6** (2024), article no. 3665.
- [23] E. F. Aboelfetoh and R. Pietschnig, "Preparation and catalytic performance of Al₂O₃, TiO₂ and SiO₂ supported vanadium based-catalysts for C–H activation", *Catal. Lett.* **127** (2009), pp. 83–94.
- [24] F. Adam, T.-S. Chew and J. Andas, "Liquid phase oxidation of acetophenone over rice husk silica vanadium catalyst", *Chin. J. Catal.* **33** (2012), pp. 518–522.
- [25] L. D. Frederickson and D. M. Hausen, "Infrared spectra-structure correlation study of vanadium-oxygen compounds", *Anal. Chem.* **35** (1963), pp. 818–827.
- [26] K. V. Narayana, B. D. Raju, S. K. Masthan, V. V. Rao, P. K. Rao and A. Martin, "Cerium fluoride supported V₂O₅ catalysts: physico-chemical characterization and 3-picoline ammoxidation activity", *J. Mol. Catal. A Chem.* **223** (2004), pp. 321–328.
- [27] T. Radhika and S. Sugunan, "Structural and catalytic investigation of vanadia supported on ceria promoted with high surface area rice husk silica", *J. Mol. Catal. A Chem.* **250** (2006), pp. 169–176.